Abstract

Throughout the history of wireless communications, spatial antenna diversity has been important in improving the radio link between wireless users. Historically, microscopic antenna diversity has been used to reduce the fading seen by a radio receiver, whereas macroscopic diversity provides multiple listening posts to ensure that mobile communication links remain intact over a wide geographic area. In recent years, the concepts of spatial diversity have been expanded to build foundations for emerging technologies, such as smart (adaptive) antennas and position location systems. Smart antennas hold great promise for increasing the capacity of wireless communications because they radiate and receive energy only in the intended directions, thereby greatly reducing interference. To properly design, analyze, and implement smart antennas and to exploit spatial processing in emerging wireless systems, accurate radio channel models that incorporate spatial characteristics are necessary. In this tutorial, we review the key concepts in spatial channel modeling and present emerging approaches. We also review the research issues in developing and using spatial channel models for adaptive antennas.

Overview of Spatial Channel Models for Antenna Array Communication Systems

Richard B. Ertel and Paulo Cardieri, Virginia Polytechnic Institute
Kevin W. Sowerby, University of Auckland, New Zealand
Theodore S. Rappaport and Jeffrey H. Reed, Virginia Polytechnic Institute

With the advent of antenna array systems for both interference cancellation and position location applications comes the need to better understand the spatial properties of the wireless communications channel. These spatial properties of the channel will have an enormous impact on the performance of antenna array systems; hence, an understanding of these properties is paramount to effective system design and evaluation.

The challenge facing communications engineers is to develop realistic channel models that can efficiently and accurately predict the performance of a wireless system. It is important to stress here that the level of detail about the environment a channel model must provide is *highly dependent* on the type of system under consideration. To predict the performance of single-sensor narrowband receivers, it may be acceptable to consider only the received signal power and/or time-varying amplitude (fading) distribution of the channel. However, for emerging wideband multisensor arrays, in addition to signal power level, information regarding the signal multipath delay and angle of arrival (AOA) is needed.

Classical models provide information about signal power level distributions and Doppler shifts of the received signals. These models have their origins in the early days of cellular radio when wideband digital modulation techniques were not readily available. As shown subsequently, many of the emerging spatial models in the literature utilize the fundamental principles of the classical channel models. However, modern spatial channel models build on the classical understanding of fading and Doppler spread, and incorporate additional concepts such as time delay spread, AOA, and adaptive array antenna geometries.

In this article, we review the fundamental channel models that have led to the present-day theories of spatial diversity from both mobile user and base station perspectives. The evolution of these models has paralleled that of cellular systems. Early models only accounted for amplitude and time-varying properties of the channel. These models were then enhanced by adding time delay spread information, which is important when dealing with digital transmission performance. Now, with the introduction of techniques and features that depend on the spatial distribution of the mobiles, spatial information is required in the channel models. As shown in the next sections, more accurate models for the distribution of the scatterers surrounding the mobile and base station are needed. The differentiation between the mobile and base station is important. Classical work has demonstrated that models must account for the physical geometry of scattering objects in the vicinity of the antenna of interest. The number and locations of these scattering objects are dependent on the heights of the antennas, particularly regarding the local environment.

This article, then, explores some of the emerging models for spatial diversity and adaptive antennas, and includes the physical mechanisms and motivations behind the models. A literature survey of existing RF channel measurements with AOA information is also included. The article concludes with a summary and suggestions for future research.

Wireless Multipath Channel Models

This section describes the physical properties of the wireless communication channel that must be modeled. In a wireless system, a signal transmitted into the channel interacts with the environment in a very complex way. There are reflections from large objects, diffraction of the electromagnetic waves

This work was partially supported by the DARPA GloMo program, Virginia Tech's Federal Highways Research Center of Excellence, Virginia Tech's Bradley Foundation, the Brazilian National Science Council — CNPq, and NSF Presidential Faculty Fellowship.

1070-9916/98/$10.00 © 1998 IEEE

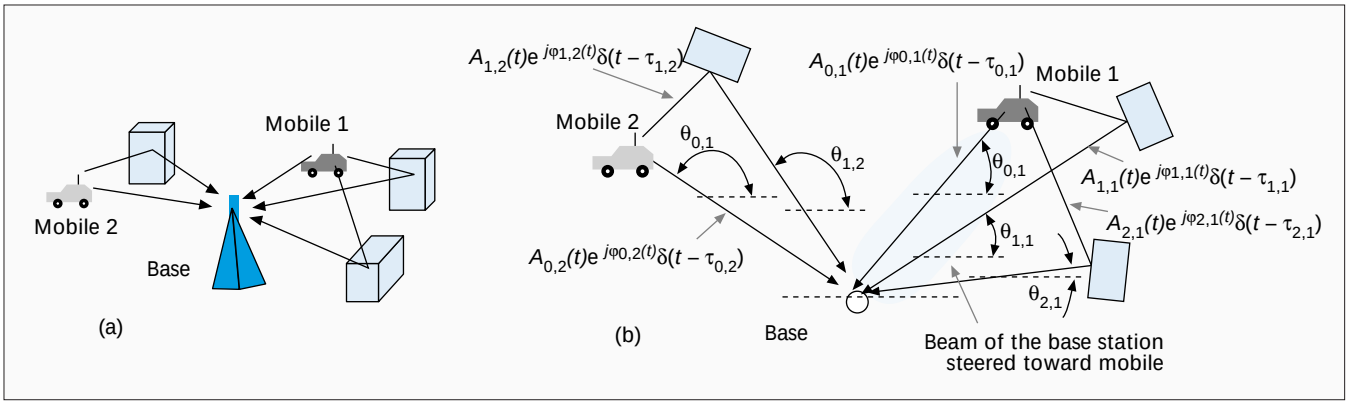

Figure 1. *Multipath propagation channel: a) side view; b) top view.*

around objects, and signal scattering. The result of these complex interactions is the presence of many signal components, or *multipath* signals, at the receiver. Another property of wireless channels is the presence of Doppler shift, which is caused by the motion of the receiver, the transmitter, and/or any other objects in the channel. A simplified pictorial of the multipath environment with two mobile stations is shown in Fig. 1. Each signal component experiences a different path environment, which will determine the amplitude $A_{l,k}$, carrier phase shift $\varphi_{l,k}$, time delay $\tau_{l,k}$, AOA $\theta_{l,k}$, and Doppler shift f_d of the lth signal component of the kth mobile. In general, each of these signal parameters will be time-varying.

The early classical models, which were developed for narrowband transmission systems, only provide information about signal amplitude level distributions and Doppler shifts of the received signals. These models have their origins in the early days of cellular radio [1–4] when wideband digital modulation techniques were not readily available.

As cellular systems became more complex and more accurate models were required, additional concepts, such as time delay spread, were incorporated into the model. Representing the RF channel as a time-variant channel and using a baseband complex envelope representation, the channel impulse response for mobile 1 has classically been represented as [5]

$$h_1(t,\tau)=\sum_{l=0}^{L(t)-1} A_{l,1}(t)e^{j\varphi_{l,1}(t)}\delta\left(t-\tau_{l,1}(t)\right) \qquad (1)$$

where $L(t)$ is the number of multipath components and the other variables have already been defined. The amplitude $A_{l,k}$ of the multipath components is usually modeled as a Rayleigh distributed random variable, while the phase shift $\varphi_{l,k}$ is uniformly distributed.

The time-varying nature of a wireless channel is caused by the motion of objects in the channel. A measure of the time rate of change of the channel is the *Doppler power spectrum*, introduced by M. J. Gans in 1972 [2]. The Doppler power spectrum provides us with statistical information on the variation of the frequency of a tone received by a mobile traveling at speed v. Based on the flat fading channel model developed by R. H. Clarke in 1968, Gans assumed that the received signal at the mobile station came from all directions and was uniformly distributed. Under these assumptions and for a $\lambda/4$ vertical antenna, the Doppler power spectrum is given by [5]

$$S(f)=\begin{cases}\dfrac{1.5}{\pi f_m\sqrt{1-\left(\dfrac{f-f_c}{f_m}\right)^2}} & |f-f_c|<f_m\\ 0 & \textit{elsewhere}\end{cases}$$

where f_m is the maximum Doppler shift given by v/λ where λ is the wavelength of the transmitted signal at frequency f_c.

Figure 2 shows the received signals at the base station, assuming that mobiles 1 and 2 have transmitted narrow pulses at the same time. Also shown is the output of an antenna array system adapted to mobile 1.

The channel model in Eq. 1 does not consider the AOA of each multipath component shown in Figs. 1 and 2. For narrowband signals, the AOA may be included into the vector channel impulse response using

$$\vec{h}_1(t,\tau)=\sum_{l=0}^{L(t)-1} A_{l,1}(t)e^{j\varphi_l(t)}\vec{a}\left(\theta_l(t)\right)\delta\left(t-\tau_l(t)\right) \qquad (2)$$

where $\vec{a}(\theta_l(t))$ is the *array response vector*. The array response vector is a function of the array geometry and AOA. Figure 3 shows the case for an arbitrary array geometry when the array and signal are restricted to two-dimensional space. The resulting array response vector is given by

$$a\left(\theta_l(t)\right)=\begin{bmatrix}\exp\left(-j\psi_{l,1}\right)\\ \exp\left(-j\psi_{l,2}\right)\\ \exp\left(-j\psi_{l,3}\right)\\ \cdots\\ \exp\left(-j\psi_{l,m}\right)\end{bmatrix}$$

where $\psi_{l,i}(t)=[x_i\cos(\theta_l(t))+y_i\sin(\theta_l(t))]\beta$ and $\beta=2\pi/\lambda$ is the wavenumber.

The spatial channel impulse response given in Eq. 2 is a summation of several multipath components, each of which has its own amplitude, phase, and AOA. The distribution of these parameters is dependent on the type of environment. In particular, the angle spread of the channel is known to be a function of both the environment and the base station antenna heights. In the next section, we describe macrocell and microcell environments and discuss how the environment affects the signal parameters.

Macrocell vs. Microcell

Macrocell Environment — Figure 4 shows the channel on the forward link for a macrocell environment. It is usually assumed that the scatterers surrounding the mobile station are about the same height as or are higher than the mobile. This implies that the received signal at the mobile antenna arrives from all directions after bouncing from the surrounding scatterers as illustrated in Fig. 4.

Under these conditions, Gans' assumption that the AOA is uniformly distributed over $[0, 2\pi]$ is valid. The classical

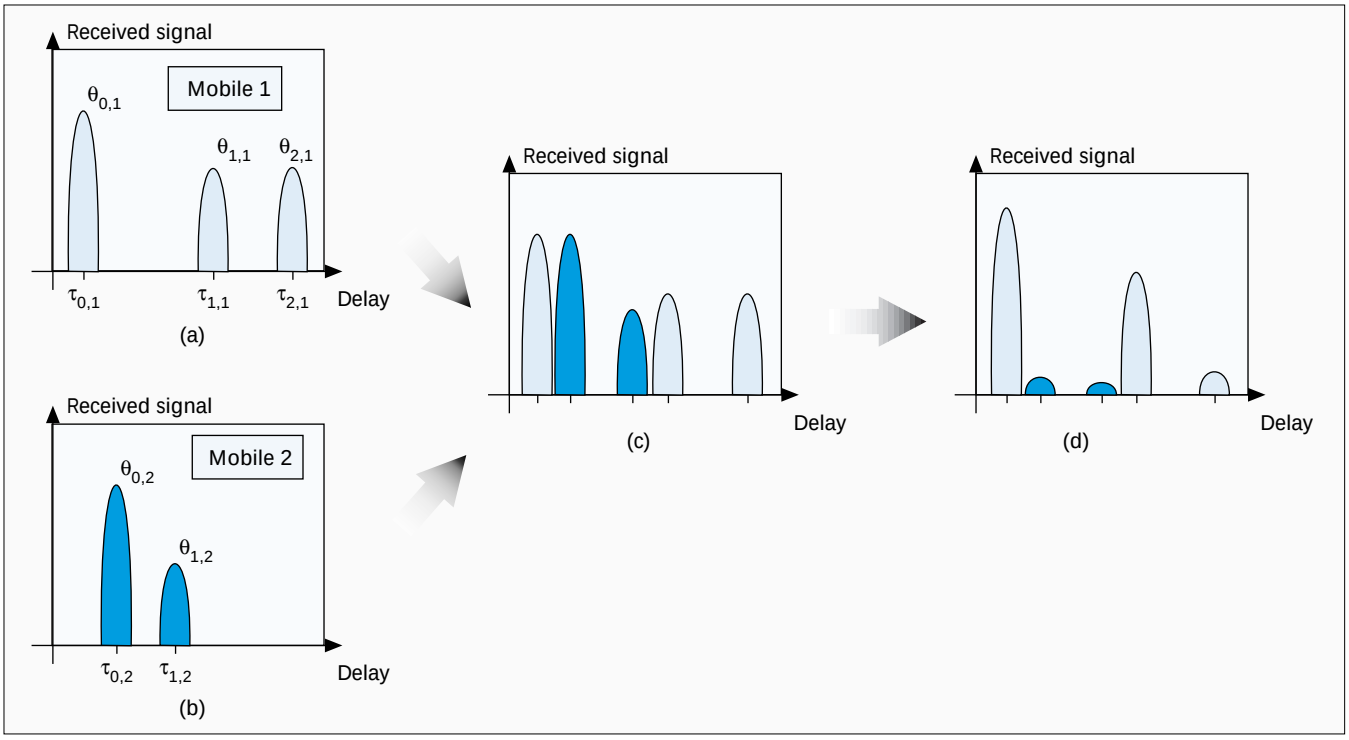

Figure 2. *Channel impulse responses for mobiles 1 and 2: a) received signal from mobile 1 to the base station; b) received signal from mobile 2 to the base station; c) combined received signal from mobiles 1 and 2 at the base station; d) received signal at the base station when a beam steered toward mobile 1 is employed.*

Rayleigh fading envelope with deep fades approximately $\lambda/2$ apart emanates from this model [5].

However, the AOA of the received signal at the base station is quite different. In a macrocell environment, typically, the base station is deployed higher than the surrounding scatterers. Hence, the received signals at the base station result from the scattering process in the vicinity of the mobile station, as shown in Fig. 5. The multipath components at the base station are restricted to a smaller angular region, θ_{BW}, and the distribution of the AOA is no longer uniform over $[0,2\pi]$. Other AOA distributions are considered later in this article.

The base station model of Fig. 5 was used to develop the theory and practice of base station diversity in today's cellular system and has led to rules of thumb for the spacing of diversity antennas on cellular towers [3].

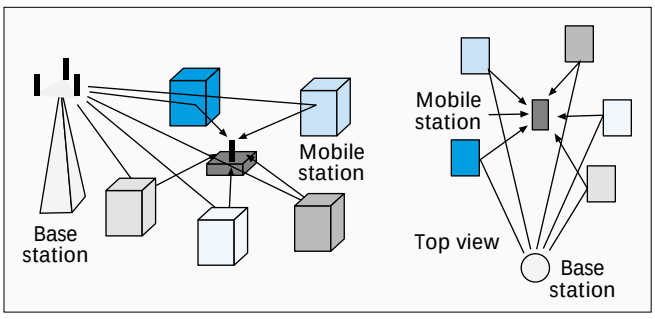

Figure 4. *Macrocell environment — the mobile station perspective.*

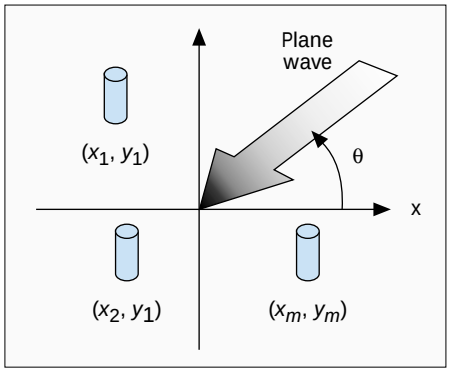

Figure 3. *Arbitrary antenna array configuration.*

Microcell Environment — In the microcell environment, the base station antenna is usually mounted at the same height as the surrounding objects. This implies that the scattering spread of the AOA of the received signal at the base station is larger than in the macrocell case since the scattering process also happens in the vicinity of the base station. Thus, as the base station antenna is lowered, the tendency is for the multipath AOA spread to increase. This change in the behavior of the received signal is very important as far as antenna array applications are concerned. Studies have shown that statistical characteristics of the received signal are functions of the angle spread. Lee [3] and Adachi [6] found that the correlation between the signals received at two base station antennas increases as the angle spread decreases.

This section has presented some of the physical properties of a wireless communication channel. A mathematical expression that describes the time-varying spatial channel impulse response was given in Eq. 2. In the next section, several models that provide varying levels of information about the spatial channel are presented.

Space: The Final Frontier

Details of the Spatial Channel Models

In the past when the distribution of angle of arrival of multipath signals was unknown, researchers assumed uniform distribution over $[0, 2\pi]$ [7]. In this section, a number of more realistic spatial channel models are introduced. The defining equations (or geometry) and the key results for the models

are described. Also provided is an extensive list of references.

Table 1 lists some representative active research groups in the field and their Web site addresses where more information on the subject can be found. (Note that this is by no means an exhaustive list.)

The Gaussian Wide Sense Stationary Uncorrelated Scattering (GWSSUS), Gaussian Angle of Arrival (GAA), Typical Urban (TU), and Bad Urban (BU) models described below were developed in a series of papers at the Royal Institute of Technology and may be downloaded from the Web site. Further details of the Geometrically Based Single Bounce (GBSB) models are given in theses at Virginia Tech, which are available at http://etd.vt.edu/etd/index.html.

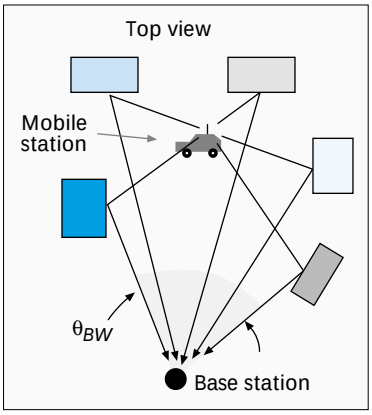

Figure 5. *Macrocell — base station perspective.*

These various models were developed and used for different applications. Some of the models were intended to provide information about only a single channel characteristic, such as angle spread, while others attempt to capture all the properties of the wireless channel. In the discussion of the models, an effort is made to identify the original motivation of the model and to convey the information the model is intended to provide.

Lee's Model

In Lee's model, scatterers are evenly spaced on a circular ring about the mobile as shown in Fig. 6. Each of the scatterers is intended to represent the effect of many scatterers within the region, and hence are referred to as *effective scatterers*. The model was originally used to predict the correlation between the signals received by two sensors as a function of element spacing. However, since the correlation matrix of the received signal vector of an antenna array can be determined by considering the correlation between each pair of elements, the model has application to any arbitrary array size.

The level of correlation will determine the performance of spatial diversity methods [3, 9]. In general, larger angle spreads and element spacings result in lower correlations, which provide an increased diversity gain. Measurements of the correlation observed at both the base station and the mobile are consistent with a narrow angle spread at the base station and a large angle spread at the mobile. Correlation measurements made at the base station indicate that the typical radius of scatterers is from 100 to 200 wavelengths [3].

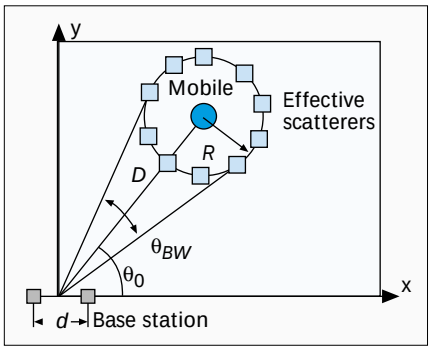

Figure 6. *Lee's model.*

Assuming that N scatterers are uniformly placed on the circle with radius R and oriented such that a scatterer is located on the line of sight, the discrete AOAs are [9]

$$\theta_i \approx \frac{R}{D}\sin\left(\frac{2\pi}{N}i\right) \text{ for } i = 0,1,\ldots,N-1.$$

From the discrete AOAs, the correlation of the signals between any two elements of the array can be found using [9]

$$\rho(d,\theta_0,R,D) = \frac{1}{N}\sum_{i=0}^{N-1}\exp\left[-j2\pi d\ \cos(\theta_0+\theta_i)\right],$$

where d is the element spacing and θ_0 is measured with respect to the line between the two elements as shown in Fig. 6.

The original model provided information regarding only signal correlations. Motivated by the need to consider small-scale fading in diversity systems, Stapleton *et al.* proposed an extension to Lee's model that accounts for Doppler shift by imposing an angular velocity on the ring of scatterers [10, 11]. For the model to give the appropriate maximum Doppler shift, the angular velocity of the scatterers must equal v/R where v is the vehicle velocity and R is the radius of the scatterer ring [11]. Using this model to simulate a Rayleigh fading spatial channel model, the BER for a $\pi/4$ differential quadrature phase shift keyed (DQPSK) signal was simulated. The results were compared with measurements taken in a typical suburban environment. The resulting BER estimates were within a factor of two of the actual measured BER, indicating a reasonable degree of accuracy for the model [10].

When the model is used to provide

Research group	Web site
Center for Communications Research — University of Bristol	http://www.fen.bris.ac.uk/elec/research/ccr/ccr.html
Center for Personkommunikation — Aalborg University	http://www.kom.auc.dk/CPK/
Center for Wireless Telecommunications — Virginia Tech	http://www.cwt.vt.edu/
Mobile and Portable Radio Research Group — Virginia Tech	http://www.mprg.ee.vt.edu
Research Group for RF Communications — University of Kaiserlautern	http://www.e-technik.uni-kl.de/
Royal Institute of Technology	http://www.s3.kth.se
Smart Antenna Research Group — Stanford University	http://www-isl.stanford.edu/groups/SARG
Telecommunications and Information Systems Engineering — University of Texas at Austin	http://www.ece.utexas.edu/projects/tise/
Wireless Technology Group — McMaster University	http://www.crl.mcmaster.ca

Table 1. *Some active research groups in the field of adaptive antenna arrays.*

joint AOA and time of arrival (TOA) channel information, one finds that the resulting power delay profile is "U-shaped" [12]. By considering the intersections of the effective scatterers by ellipses of constant delay, one finds that there is a high concentration of scatterers in ellipses with minimum delay, a high concentration of scatterers in ellipses with maximum delay, and a lower concentration of scatterers between. Higher concentrations of scatterers with a given delay correspond with larger powers, and hence larger values on the power delay profile. The "U-shaped" power delay profile is not consistent with measurements. Therefore, an extension to Lee's model is proposed in [11] in which additional scatterer rings are added to provide different power delay profiles.

While the model is quite useful in predicting the correlation between any two elements of the array, and hence the array correlation matrix, it is not well suited for simulations requiring a complete model of the wireless channel.

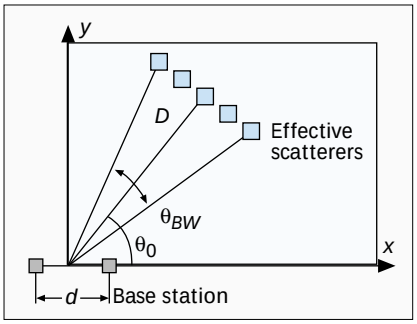

Figure 7. *Discrete uniform geometry.*

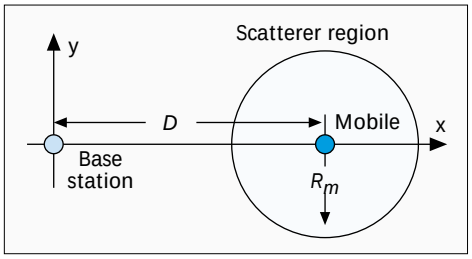

Figure 8. *Circular scatterer density geometry.*

Discrete Uniform Distribution

A model similar to Lee's model in terms of both motivation and analysis was proposed in [9]. The model (referred to here as the discrete uniform distribution) evenly spaces N scatterers within a narrow beamwidth centered about the line of sight to the mobile as shown in Fig. 7. The discrete possible AOAs, assuming N is odd, are given by [9]

$$\theta_i = \frac{1}{N-1}\theta_{BW} i, \quad i = -\frac{N-1}{2}, \ldots, \frac{N-1}{2}.$$

From this, the correlation of the signals present at two antenna elements with a separation of d is found to be

$$\rho(d, \theta_0, \theta_{BW}) = \frac{1}{N} \sum_{i=-\frac{N-1}{2}}^{\frac{N-1}{2}} \exp\left[-j2\pi d \cos(\theta_0 + \theta_i)\right].$$

Measurements reported in [9] suggest that the AOA statistics in rural and suburban environments are Gaussian distributed (see the discussion of the GAA model later). However, in practice the AOA will be discrete (i.e., a finite number of samples from a Gaussian distribution), and therefore it is not valid to use a continuous AOA distribution to estimate the correlation present between different antenna elements in the array. The correlation that results from a continuous AOA distribution decreases monotomically with element spacing, whereas the correlation that results from a discrete AOA has damped oscillations present. Therefore, a continuous AOA distribution will underestimate the correlation that exists between the elements in the array [9].

In [9], a comparison is made between the correlation obtained using the discrete uniform distribution model, Lee's model, and a continuous Gaussian AOA as a function of element spacing. The comparisons indicate that, for small element separations (two wavelengths), the three models have nearly identical correlations. For larger element separations (greater than two wavelengths), the correlation values using the continuous Gaussian AOA are close to zero, while the two discrete models have oscillation peaks with correlations as high as 0.2 even beyond four wavelengths. Additionally, it was found that the correlation of the discrete uniform distribution falls off more quickly than the correlation in Lee's model.

Again, while the model is useful for predicting the correlation between any pair of elements in the array (which can be used to calculate the array correlation matrix), it fails to include all the phenomena, such as delay spread and Doppler spread, required for certain types of simulations.

Geometrically Based Single-Bounce Statistical Channel Models

Geometrically Based Single-Bounce (GBSB) Statistical Channel Models are defined by a spatial scatterer density function. These models are useful for both simulation and analysis purposes. Use of the models for simulation involves randomly placing scatterers in the scatterer region according to the form

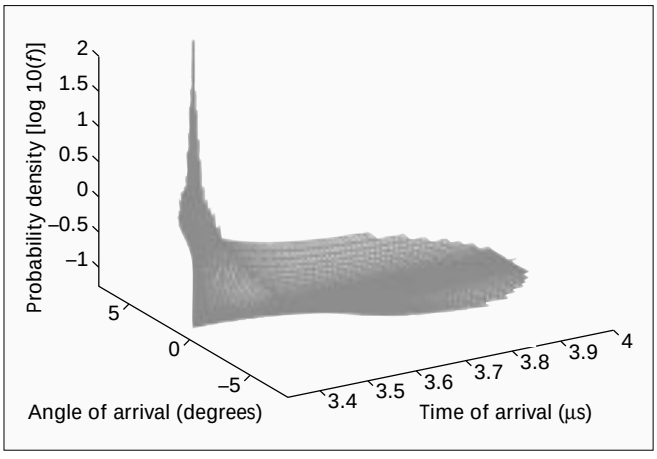

Figure 9. *Joint TOA and AOA probability density function at the base station, circular model (log-scale).*

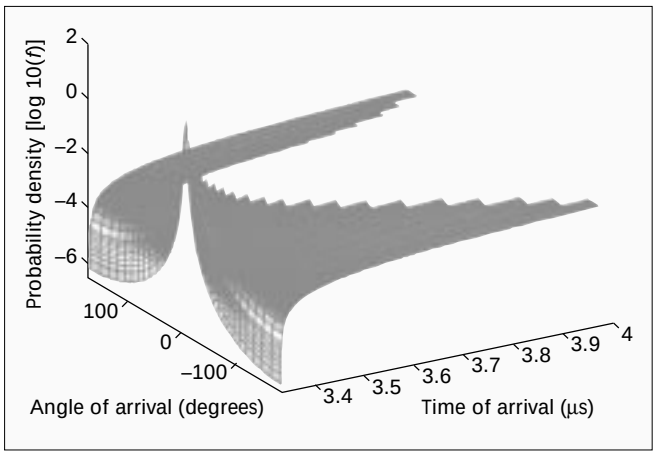

Figure 10. *Joint TOA and AOA probability density function at the mobile, circular model (log-scale).*

of the spatial scatterer density function. From the location of each of the scatterers, the AOA, TOA, and signal amplitude are determined.

From the spatial scatterer density function, it is possible to derive the joint and marginal TOA and AOA probability density functions. Knowledge of these statistics can be used to predict the performance of an adaptive array. Furthermore, knowledge of the underlying structure of the resulting array response vector may be exploited by beamforming and position location algorithms.

The shape and size of the spatial scatterer density function required to provide an accurate model of the channel is subject to debate. Validation of these models through extensive measurements remains an active area of research.

Geometrically Based Circular Model (Macrocell Model) — The geometry of the Geometrically Based Single Bounce Circular Model (GBSBCM) is shown in Fig. 8. It assumes that the scatterers lie within radius R_m about the mobile. Often the requirement that $R_m < D$ is imposed. The model is based on the assumption that in macrocell environments where antenna heights are relatively large, there will be no signal scatterering from locations near the base station. The idea of a circular region of scatterers centered about the mobile was originally proposed by Jakes [13] to derive theoretical results for the correlation observed between two antenna elements. Later, it was used to determine the effects of beamforming on the Doppler spectrum [14, 15] for narrowband signals. It was shown that the rate and the depth of the envelope fades are significantly reduced when a narrow-beam beamformer is used.

The joint TOA and AOA density function obtained from the model provides some insights into the properties of the model. Using a Jacobian transformation, it is easy to derive the joint TOA and AOA density function at both the base station and the mobile. The resulting joint probability density functions (PDFs) at the base station and the mobile are shown in the box on this page [16].

The joint TOA and AOA PDFs for the GBSBCM are shown in Figs. 9 and 10 for the case of D = 1 km and R_m = 100 m from the base station and mobile perspectives, respectively. The circular model predicts a relatively high probability of multipath components with small excess delays along the line of sight. From the base-station perspective, all of the multipath components are restricted to lie within a small range of angles.

The appropriate values for the radius of scatterers can be determined by equating the angle spread predicted by the model (which is a function of R_m) with measured values. Measurements reported in [9] suggest that typical angle spreads for macrocell environments with a T-R separation of 1 km are approximately two to six degrees. Also, it is stated that the angle spread is inversely proportional to the T-R separation, which leads to a radius of scatterers that ranges from 30 to 200 m [16]. In [3], it is stated that the active scattering region around the mobile is about 100–200 wavelengths for 900 MHz, which provides a range of 30–60 m, roughly the width of wide urban streets.

The GBSBCM can be used to generate random channels for simulation purposes. Generation of samples from the GBSBCM is accomplished by uniformly placing scatterers in the circular scatterer region about the mobile and then calculating the corresponding AOA, TOA, and power levels.

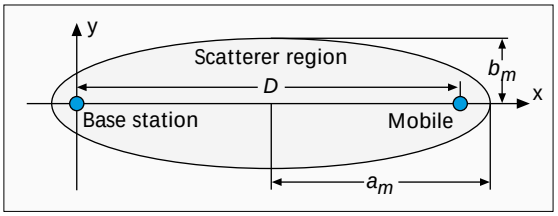

Figure 11. *Elliptical scatterer density geometry.*

Geometrically Based Elliptical Model (Microcell Wideband Model) — The Geometrically Based Single Bounce Elliptical Model (GBSBEM) assumes that scatterers are uniformly distributed within an ellipse, as shown in Fig. 11, where the base station and mobile are the foci of the ellipse. The model was proposed for microcell environments where antenna heights are relatively low, and therefore multipath scattering near the base station is just as likely as multipath scatterering near the mobile [17, 18].

A nice attribute of the elliptical model is the physical interpretation that only multipath signals which arrive with an absolute delay $\leq \tau_m$ are accounted for by the model. Ignoring components with larger delays is possible since signals with longer delays will experience greater path loss, and hence have relatively low power compared to those with shorter delays. Therefore, provided that τ_m is chosen sufficiently large, the model will account for nearly all the power and AOA of the multipath signals.

The parameters a_m and b_m are the semimajor axis and semiminor axis values, which are given by

$$a_m = \frac{c\tau_m}{2},$$

$$b_m = \frac{1}{2}\sqrt{c^2{\tau_m}^2 - D^2},$$

At the base station:

$$f_{\tau,\theta_b}(\tau,\theta_b) =$$

$$\begin{cases} \dfrac{\left(D^2-\tau^2c^2\right)\left(D^2c+\tau^2c^3-2\tau c^2D\cos(\theta_b)\right)}{4\pi R_m^2\left(D\cos(\theta_b)-\tau c\right)^3} & : \quad \dfrac{D^2-2\tau cD\cos(\theta_b)+\tau^2c^2}{\tau c-D\cos(\theta_b)} \leq 2R_m \\ 0 & : \quad \textit{else.} \end{cases}$$

At the mobile:

$$f_{\tau,\theta_m}(\tau,\theta_m) =$$

$$\begin{cases} \dfrac{\left(D^2-\tau^2c^2\right)\left(D^2c+\tau^2c^3-2\tau c^2D\cos(\theta_m)\right)}{4\pi R_m^2\left(D\cos(\theta_m)-\tau c\right)^3} & : \quad \dfrac{D^2-\tau^2c^2}{D\cos(\theta_m)-\tau c} \leq 2R_m \\ 0 & : \quad \textit{else,} \end{cases}$$

where θ_b and θ_m are the angle of arrival measured relative to the line of sight from the base station and the mobile, respectively.

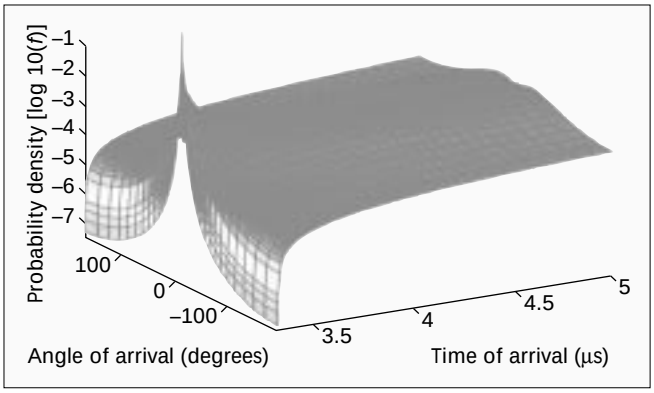

Figure 12. *Joint TOA and AOA probability density function, elliptical model (log-scale).*

where c is the speed of light and τ_m is the maximum TOA to be considered. To gain some insight into the properties of this model, consider the resulting joint TOA and AOA density function. Using a transformation of variables of the original uniform scatterer spatial density function, it can be shown that the joint TOA and AOA density function observed at the base station is given by [16]

$$f_{\tau,\theta_b}(\tau,\theta_b) = \begin{cases} \dfrac{\left(D^2-\tau^2c^2\right)\left(D^2c+\tau^2c^3-2\tau c^2 D\cos(\theta_b)\right)}{4\pi a_m b_m\left(D\cos(\theta_b)-\tau c\right)^3} & \dfrac{D}{c} \le \tau \le \tau_m \\ 0 & \text{elsewhere,} \end{cases}$$

where θ_b is AOA observed at the base station. A plot of the joint TOA and AOA PDF is shown in Fig. 12 for the case of D = 1 km and τ_m = 5 μs. From the plot of the joint TOA and AOA PDF, it is apparent that the GBSBEM results in a high probability of scatterers with minimum excess delay along the line of sight.

The choice of τ_m will determine both the delay spread and angle spread of the channel. Methods for selecting an appropriate value of τ_m are given in [18]. Table 2 summarizes the techniques for selecting τ_m where L_r is the reflection loss in dB, n is the path loss exponent, and τ_0 is the minimum path delay.

To generate multipath profiles using the GBSBEM, the most efficient method is to uniformly place scatterers in the ellipse and then calculate the corresponding AOA, TOA, and power levels from the coordinates of the scatterer. Uniformly placing scatterers in an ellipse may be accomplished by first uniformly placing the scatterers in a unit circle and then scaling each x and y coordinate by a_m and b_m, respectively [16].

Gaussian Wide Sense Stationary Uncorrelated Scattering

The GWSSUS is a statistical channel model that makes assumptions about the form of the received signal vector [19–22]. The primary motivation of the model is to provide a general equation for the received signal correlation matrix. In the GWSSUS model, scatterers are grouped into clusters in space. The clusters are such that the delay differences within each cluster are not resolvable within the transmission signal bandwidth. By including multiple clusters, frequency-selective fading channels can be modeled using the GWSSUS. Figure 13 shows the geometry assumed for the GWSSUS model corresponding to d = 3 clusters. The mean AOA for the kth cluster is denoted θ_{0k}. It is assumed that the location and delay associated with each cluster remains constant over several data bursts, b. The form of the received signal vector is

$$\mathbf{x}_b(t) = \sum_{k=1}^{d} \mathbf{v}_{k,b}\, s(t-\tau_k),$$

where $v_{k,b}$ is the superposition of the steering vectors during the bth data burst within the kth cluster, which may be expressed as

$$\mathbf{v}_{k,b} = \sum_{i=1}^{N_k} \alpha_{k,i} e^{j\phi_{k,i}}\, \mathbf{a}\left(\theta_{0k}-\theta_{k,i}\right),$$

where N_k denotes the number of scatterers in the kth cluster, $\alpha_{k,i}$ is the amplitude, $\phi_{k,j}$ is the phase, $\theta_{k,i}$ is the angle of arrival of the ith reflected scatterer of the kth cluster, and $\mathbf{a}(\theta)$ is the array response vector in the direction of θ [9]. It is assumed that the steering vectors are independent for different k.

If N_k is sufficiently large (approximately 10 or more [19]) for each cluster of scatterers, the central limit theorem may be applied to the elements of $\mathbf{v}_{k,b}$. Under this condition, the elements of $\mathbf{v}_{k,b}$ are Gaussian distributed. Additionally, it is assumed that $\mathbf{v}_{k,b}$ is wide sense stationary. The time delays τ_k are assumed to be constant over several bursts, b, whereas the phases $\phi_{k,i}$ change much more rapidly. The vectors $\mathbf{v}_{k,b}$ are assumed to be zero mean, complex Gaussian wide sense, stationary random processes where b plays the role of the time argument. The vector $\mathbf{v}_{k,b}$ is a multivariate Gaussian distribution, which is described by its mean and covariance matrix. When no line of sight component is present, the mean will be zero due to the random phase $\phi_{k,i}$, which is assumed to be uniformly distributed in the range 0 to 2π. When a direct path component is present, the mean becomes a scaled version of the corresponding array response vector $E\{\mathbf{v}_{k,b}\} \propto \mathbf{a}(\theta_{0k})$ [9]. The covariance matrix for the kth cluster is given by [21]

$$R_k = E\left\{\mathbf{v}_{k,b}\mathbf{v}_{k,b}^H\right\} = \sum_{i=1}^{N_k} \left|\alpha_{k,i}\right|^2 E\left\{\mathbf{a}\left(\theta_{0k}-\theta_{k,i}\right)\mathbf{a}^H\left(\theta_{0k}-\theta_{k,i}\right)\right\}.$$

The model provides a fairly general result for the form of the covariance matrix. However, it does not indicate the number or location of the scattering clusters, and hence requires some additional information for application to typical environments.

Criteria	Expression
Fixed maximum delay, τ_m	τ_m = constant
Fixed threshold T in dB	$\tau_m = \tau_0 10^{(T-Lr)/10n}$
Fixed delay spread, σ_t	$\tau_m = 3.244\sigma_\tau + \tau_0$
Fixed max. excess delay, τ_e	$\tau_m = \tau_0 + \tau_e$

Table 2. *Methods for selection* τ_m.

Gaussian Angle of Arrival

The Gaussian Angle of Arrival (GAA) channel model is a special case of the GWSSUS model described above where only a single cluster is considered (d = 1), and the AOA statistics are assumed to be Gaussian distributed about some nominal angle, θ_0, as shown in Fig. 14. Since only a single cluster is considered, the model is a narrowband channel model that is valid when the time spread of the channel is small compared to the inverse of the signal bandwidth; hence, time shifts may be modeled as simple phase shifts [23].

The statistics of the steering vector are distributed as a multivariate Gaussian random variable. Similar to the GWSSUS model, if no line of

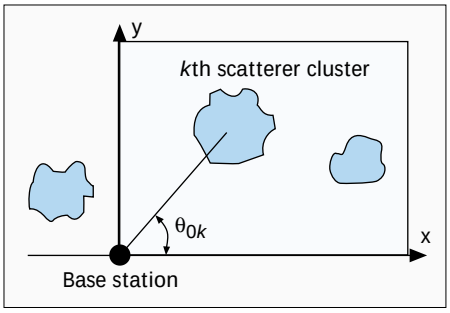

Figure 13. *GWSSUS geometry.*

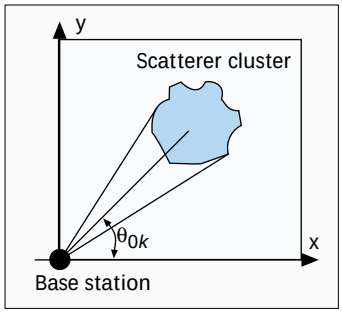

Figure 14. *GAA geometry.*

sight is present, then $E\{\mathbf{v}_{k,b}\} = 0$; otherwise, the mean is proportional to the array response vector $\mathbf{a}(\theta_{0k})$. For the special case of uniform linear arrays, the covariance matrix may be described by

$$\mathbf{R}(\theta_0, \sigma_\theta) \approx p\mathbf{a}(\theta_0)\mathbf{a}^H(\theta_0) \otimes \mathbf{B}(\theta_0, \sigma_\theta),$$

where the (k,l) element of $\mathbf{B}(\theta_0, \sigma_\theta)$ is given by

$$B(\theta_0, \sigma_\theta)_{kl} = \exp\left[-2\left(\pi\Delta(k-l)\right)^2 \sigma_\theta^2 \cos^2\theta\right],$$

p is the receiver signal power, Δ is the element spacing, and $\otimes$ denotes element-wise multiplication [23].

Time-Varying Vector Channel Model (Raleigh's Model)

Raleigh's time-varying vector channel model was developed to provide both small scale Rayleigh fading and theoretical spatial correlation properties [24]. The propagation environment considered is densely populated with large dominant reflectors (Fig. 15). It is assumed that at a particular time the channel is characterized by L dominant reflectors. The received signal vector is then modeled as

$$\mathbf{x}(t) = \sum_{l=0}^{L(t)-1} \mathbf{a}(\theta_l)\alpha_l(t)s(t-\tau) + \mathbf{n}(t),$$

where $\mathbf{a}$ is the array response vector, $\alpha_l(t)$ is the complex path amplitude, $s(t)$ is the modulated signal, and $\mathbf{n}(t)$ is additive noise. This is equivalent to the impulse response given in Eq. 2.

The unique feature of the model is in the calculation of the complex amplitude term, $a_l(t)$, which is expressed as

$$\alpha_1(t) = \beta_l(t) \cdot \sqrt{\Gamma_l \cdot \psi(\tau_l)},$$

where Γ_l accounts for log-normal fading, $\psi(\tau_l)$ describes the power delay profile, and $\beta_l(t)$ is the complex intensity of the radiation pattern as a function of time. The complex intensity is described by

$$\beta_l(t) = K\sum_{n=1}^{N_l} C_n(\theta_l)\exp\left(j\omega_d \cos(\Omega_{n,l})t\right),$$

where N_l is the number of signal components contributing to the lth dominant reflecting surface, K accounts for the antenna gains and transmit signal power, $C_n(\theta_l)$ is the complex radiation of the nth component of the lth dominant reflecting surface in the direction of θ_l, ω_d is the maximum Doppler shift, and $\Omega_{n,l}$ is the angle toward the nth component of the lth dominant reflector with respect to the motion of the mobile. The resulting complex intensity, $\beta_l(t)$, exhibits a complex Gaussian distribution in all directions away from the mobile [24].

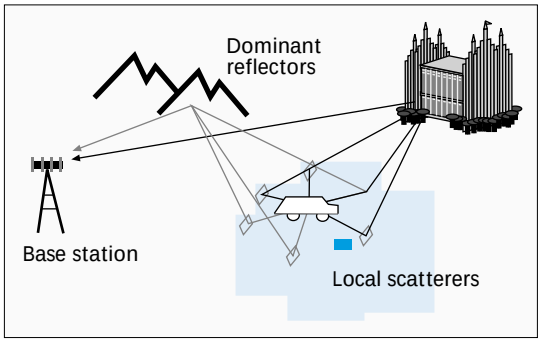

Figure 15. *Raleigh's model signal environment.*

Both the time and spatial correlation properties of the model are compared to theoretical results in [24]. The comparison shows that there is good agreement between the two.

Two Simulation Models (TU and BU)

Next we describe two spatial channel models that have been developed for simulation purposes.

The Typical Urban (TU) model is designed to have time properties similar to the GSM-TU defined in GSM 05.05, while the Bad Urban (BU) model was developed to model environments with large reflectors that are not in the vicinity of the mobile. Although the models are designed for GSM, DCS1800, and PCS1900 formats, extensions to other formats are possible [251].

Both of these models obtain the received signal vector using

$$\mathbf{x}(t) = \sum_{n=1}^{N} \alpha_n(t)\exp\left(-j2\pi f_c \frac{l_n(t)}{c} + \beta\right)s\left(t - \frac{l_n(t)}{c} + \Delta_t\right)\mathbf{a}\left(\theta_n(t)\right)$$

where N is the number of scatterers, f_c the carrier frequency, c is the speed of light, $l_n(t)$ the path propagation distance, β a random phase, and Δ_t random delay. In general, the path propagation distance $l_n(t)$ will vary continuously with time; hence, Doppler fading occurs naturally in the model.

Typical Urban (TU) — In the TU model, 120 scatterers are randomly placed within a 1 km radius about the mobile [25]. The position of the scatterers is held fixed over the duration in which the mobile travels a distance of 5 m. At the end of the 5 m, the scatterers are returned to their original position with respect to the mobile. At each 5-m interval, random phases are assigned to the scatterers as well as randomized shadowing effects, which are modeled as log-normal with distance with a standard deviation of 5–10 dB [25]. The received signal is determined by brute force from the location of each of the scatterers. An exponential path loss law is also applied to account for large-scale fading [21]. Simulations have shown that the TU model and the GSM-TU model have nearly identical power delay profiles, Doppler spectrums, and delay spreads [25]. Furthermore, the AOA statistics are approximately Gaussian and similar to those of the GAA model described above.

Bad Urban (BU) — The BU is identical to the TU model with the addition of a second scatterer cluster with another 120 scatterers offset 45° from the first, as shown in Fig. 16. The scatterers in the second cluster are assigned 5 dB less average power than the original cluster [25]. The presence of the second cluster results in an increased angle spread, which in turn reduces the off-diagonal elements of the array covariance matrix. The presence of the second cluster also causes an increase in the delay spread.

Uniform Sectored Distribution

The defining geometry of Uniform Sectored Distribution (USD) is shown in Fig. 17 [26]. The model assumes that scatterers are uniformly distributed within an angle distribution of θ_{BW} and a radial

range of ΔR centered about the mobile. The magnitude and phase associated with each scatterer is selected at random from a uniform distribution of [0,1] and [0, 2π], respectively. As the number of scatterers approaches infinity, the signal fading envelope becomes Rayleigh with uniform phase [26]. In [26], the model is used to study the effect of angle spread on spatial diversity techniques. A key result is that beam-steering techniques are most suitable for scatterer distributions with widths slightly larger than the beamwidths.

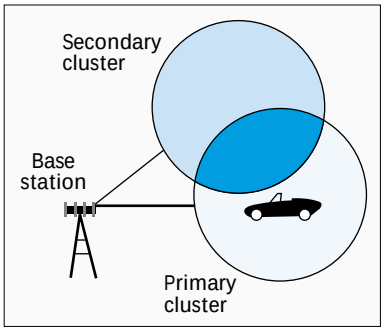

Figure 16. *Bad Urban vector channel model geometry.*

Modified Saleh-Valenzuela's Model

Saleh and Valenzuela developed a multipath channel model for indoor environment based on the clustering phenomenon observed in experimental data [27]. The clustering phenomenon refers to the observation that multipath components arrive at the antenna in groups. It was found that both the clusters and the rays within a cluster decayed in amplitude with time. The impulse response of this model is given by

$$h(t) = \sum_{i=0}^{\infty}\sum_{j=0}^{\infty}\alpha_{ij}\delta\left(t - T_i - \tau_{ij}\right) \qquad (3)$$

where the sum over i corresponds to the clusters and the sum over j represents the rays within a cluster. The variables α_{ij} are Rayleigh distributed with the mean square value described by a double-exponential decay given by

$$\overline{\alpha_{ij}^2} = \overline{\alpha_{00}^2}\exp\left(-T_i/\Gamma\right)\exp\left(\tau_{ij}/\gamma\right)$$

where Γ and γ are the cluster and ray time decay constant, respectively. Motivated by the need to include AOA in the channel mode, Spencer *et al.* proposed an extension to the Saleh-Valenzuela's model [28], assuming that time and the angle are statistically independent, or

$$h(t,\theta) = h(t)h(\theta).$$

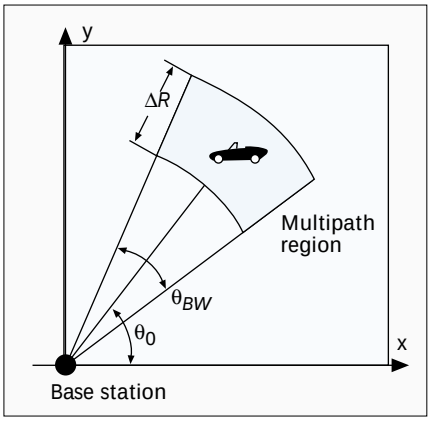

Figure 17. *Geometry of the uniform sectored distribution.*

Similar to the time impulse response in Eq. 3, the proposed *angular impulse response* is given by

$$h(t) = \sum_{i=0}^{\infty}\sum_{j=0}^{\infty}\alpha_{ij}\delta\left(\theta - \Theta_i - \omega_{ij}\right)$$

where α_{ij} is the amplitude of the jth ray in the ith cluster. The variable Θ_i is the mean angle of the ith cluster and is assumed to be uniformly distributed over [0, 2π]. The variable ω_{ij} corresponds to the ray angle within a cluster and is modeled as a Laplacian distributed random variable with zero mean and standard deviation σ:

$$f(\omega) = \frac{1}{\sqrt{2}\sigma}\exp\left(-\left|\frac{\sqrt{2}\omega}{\sigma}\right|\right).$$

This model was proposed based on indoor measurements which will be discussed in the fourth section.

Extended Tap-Delay-Line Model

A wideband channel model that is an extension of the traditional statistical tap-delay-line model and includes AOA information was developed by Klein and Mohr [29]. The channel impulse response is represented by

$$h(\tau,t,\theta) = \sum_{w=1}^{W} a_w(t)\delta\left(\tau - \tau_w\right)\delta\left(\theta - \theta_w\right).$$

This model is composed by W taps, each with an associated time delay τ_w, complex amplitude α_w, and AOA θ_w. The joint density functions of the model parameters should be determined from measurements. As shown in [29], measurements can provide histograms of the joint distribution of $|a|$, τ, and θ, and the density functions, which are proportional to these histograms, can be chosen.

Elliptical Subregions Model (Lu, Lo, and Litva's Model)

Lu *et al.* [30] proposed a model of multipath propagation based on the distribution of the scatterers in elliptical subregions, as shown in Fig. 18. Each subregion (shown in a different shade) corresponds to one range of the excess delay time. This approach is similar to the GBSBEM proposed by Liberti and Rappaport [18] in that an ellipse of scatterers is considered. The primary difference between the two models is in the selection of the number of scatterers and the distribution of those scatterers. In the GBSBEM, the scatterers were uniformly distributed within the entire ellipse. In Lu, Lo, and Litva's model, the ellipse is first subdivided into a number of elliptical subregions. The number of scatterers within each subregion is then selected from a Poisson random variable, the mean of which is chosen to match the measured time delay profile data.

It was also assumed that the multipath components arrive in clusters due to the multiple reflecting points of the scatterers. Thus, assuming that there are L scatterers with K_l reflecting points each, the model proposed is represented by

$$h(t,t_0) = \sum_{i=1}^{L} E_t\left(\theta_i^{(t)}\right) \times \sum_{k=0}^{K_i}\alpha_{ik}\exp\left(-\left(2\pi f_{ik}t_0 + \gamma_{ik}\right)\right)\delta\left(t - \tau_{ik}\right)E_r\left(\theta_{ik}\right)$$

where α_{ik}, τ_{ik}, and γ_{ik} correspond to the amplitude, time delay, and phase of the signal component from the ikth reflecting point, respectively. f_{ik} is the Doppler frequency shift of each individual path, θ_{ik} is the angle between the ikth path and the receiver-to-transmitter direction, and $\theta_i^{(t)}$ is the angle of the ith scatterer as seen from the transmitter. $E_t(\theta)$ and $E_r(\theta)$ are the radiation patterns of the transmit and receive antennas, respectively. The variable θ_{ik} was assumed to be Gaussian distributed.

Simulation results using this model were presented in [30], showing that a 60° beamwidth antenna reduces the mean RMS delay spread by about 30–43 percent. These results are consistent with similar measurements made in Toronto using a sectorized antenna [31].

Measurement-Based Channel Model

A channel model in which the parameters are based on measurement was proposed by Blanz et al. [32]. The idea behind this approach is to characterize the propagation environment, in terms of scattering points, based on measurement data. The time-variant impulse response takes the form

$$h(\tau,t) = \int_0^{2\pi} \vartheta(\tau,t,\theta) * g(\tau,\theta) * f(\tau) d\theta$$

where $f(\tau)$ is the impulse response representing the joint transfer characteristic of the transmission system components (modulator, demodulator, filters, etc.), and $g(\tau, \theta)$ is the characteristic of the base station antenna. The term $\vartheta(\tau, t, \theta)$ is the time-variant directional distribution of channel impulse response seen from the base station. This distribution is time-variant due to mobile motion and depends on the location, orientation, and velocity of the mobile station antenna and the topographical and morphographical properties of the propagation area as well. Measurement is used to determine the distribution $\vartheta(\tau, t, \theta)$.

Ray Tracing Models

The models presented so far are based on statistical analysis and measurements, and provide us with the average path loss and delay spread, adjusting some parameters according to the environment (indoor, outdoor, obstructed, etc.). In the past few years, a *deterministic* model, called *ray tracing*, has been proposed based on the geometric theory and reflection, diffraction, and scattering models. By using site-specific information, such as building databases or architecture drawings, this technique deterministically models the propagation channel [33–36], including the path loss exponent and the delay spread. However, the high computational burden and lack of detailed terrain and building databases make ray tracing models difficult to use. Although some progress has been made in overcoming the computational burden, the development of an effective and efficient procedure for generating terrain and building data for ray tracing is still necessary.

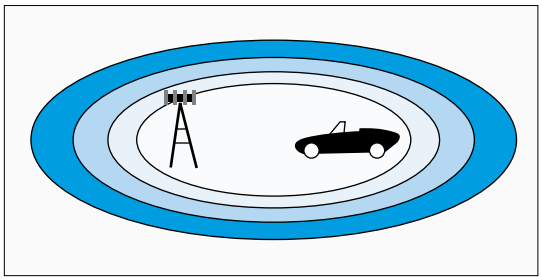

Figure 18. *Elliptical subregions spatial scatterer density.*

Channel Model Summary

Table 3 summarizes each of the spatial models presented above.

Spatial Signal Measurements

There have been only a few publications relating to spatial channel measurements. In this section, references are given to these papers, and the key results are described.

In [38], TOA and AOA measurements are presented for outdoor macrocellular environments. The measurements were made using a rotating 9° azimuth beam directional receiver antenna with a 10 MHz bandwidth centered at 1840 MHz. Three environments near Munich were considered, including rural, suburban, and urban areas with base station antenna heights of 12.3 m, 25.8 m, and 37.5 m, respectively. The key observations made include [38]:

- Most of the signal energy is concentrated in a small interval of delay and within a small AOA in rural, suburban, and even many urban environments.
- By using directional antennas, it is possible to reduce the time dispersion.

Another set of TOA and AOA measurements is reported in [39] for urban areas. The measurements were made using a two-element receiver that was mounted on the test vehicle with an elevation of 2.6 m. The transmitting antenna was placed 30 m high on the side of a building. A bandwidth of 10 MHz with a carrier frequency of 2.33 GHz was used. The delay-Doppler spectra observed at the mobile was used to obtain the delay-AOA spectra. The second antenna element is used to remove the ambiguity in AOA that would occur if only the Doppler spectra were known. The results indicate that it is possible to account for most of the major features of the delay-AOA spectra by considering the large buildings in the environment.

Motivated by diversity combining methods, earlier measurements were concerned primarily with determining the correlation between the signals at two antenna elements as a function of the element separation distance. These studies found that, at the mobile, relatively small separation distances were required to obtain a small degree of correlation between the elements, whereas at the base station very large spacing was needed. These findings indicate that there is a relatively small angle spread observed at the base station [6].

Previously, an extension to Saleh-Valenzuela's indoor model, including AOA information, was presented. This extension was proposed based on indoor measurements of delay spread and AOA at 7 GHz made at Brigham Young University [40]. The AOAs were measured using a 60 cm parabolic dish antenna that had a 3 dB beamwidth of 6°. The results showed a clustering pattern in both time and angle domain, which led to the proposed channel model described in [28]. Also, it was observed that the cluster mean angle of arrival was uniformly distributed [0, 2π]. The distribution of the angle of arrival of the rays within a cluster presented a sharp peak at the mean, leading to the Laplacian distribution modeling. The standard deviation found for this distribution was around 25°. Based on these measurements, a channel model including delay spread and AOA information was proposed, supposing that time and angle were independent variables.

In [41], two-dimensional AOA and delay spread measurement and estimation were presented. The measurements were made in downtown Paris using a channel sounder at 900 MHz and a horizontal rectangular planar array at the receiver. The estimation of AOA, including azimuth and elevation angle, was performed using 2D unitary ESPRIT [42] with a time resolution of 0.1μs and angle resolution of 5°. The results presented confirmed assumptions made in urban propagation, such as the wave-guiding mechanism of streets and the exponential decay of the power delay profile. Also, it was observed that 90 percent of the received power was contained in the paths with elevation between 0° and 40° with the low elevated paths contributing a larger amount.

Finally, in [43] measurements are used to show the variation in the spatial signature with both time and frequency. Two measures of change are given, the relative angle change given by

Model	Description	References
Lee's Model	Effective scatterers are evenly spaced on a circular ring about the mobile Predicts correlation coefficient using a discrete AOA model Extension accounts for Doppler shift	[3, 9, 11]
Discrete Uniform Distribution	*N* scatterers are evenly spaced over an AOA range Predicts correlation coefficient using a discrete AOA model Correlation predicted by this model falls off more quickly than the correlation in Lee's model	[9]
Geometrically Based Circular Model (Macrocell Model)	Assumes that the scatterers lie within circular ring about the mobile AOA, TOA, joint TOA and AOA, Doppler shift, and signal amplitude information is provided Intended for macrocell environments where antenna heights are relatively large	[12–14, 16, 37]
Geometrically Based Elliptical Model (Microcell Wideband Model)	Scatterers are uniformly distributed in an ellipse where the base station and the mobile are the foci of the ellipse AOA, TOA, joint TOA and AOA, Doppler shift, and signal amplitude information is provided Intended for microcell environments where antenna heights are relatively low	[17, 18]
Gaussian Wide Sense Stationary Uncorrelated Scattering (GWSSUS)	*N* scatterers are grouped into clusters in space such that the delay differences within each cluster are not resolvable within the transmission signal BW Provides an analytical model for the array covariance matrix	[19–22]
Gaussian Angle of Arrival (GAA)	Special case of the GWSSUS model with a single cluster and angle of arrival statistics assumed to be Gaussian distributed about some nominal angle Narrowband channel model Provides an analytical model for the array covariance matrix	[23]
Time-Varying Vector Channel Model (Raleigh's Model)	Assumes that the signal energy leaving the region of the mobile is Rayleigh faded Angle spread is accounted for by dominant reflectors Provides both Rayleigh fading and theoretical spatial correlation properties	[20]
Typical Urban	Simulation model for GSM, DCS1800, and PCS1900 Time domain properties are similar to the GSM-TU defined in GSM 05.05 120 scatterers are randomly placed within a 1 km radius about the mobile Received signal is determined by brute force from the location of each of the scatterers and the time-varying location of the mobile AOA statistics are approximately Gaussian	[21, 22, 25]
Bad Urban	Simulation model for GSM, DCS1800, and PCS1900 Accounts for large reflectors not in the vicinity of the mobile Identical to the TU model with the addition of a second scatterer cluster offset 45° from the first	[21, 22, 25]
Uniform Sectored Distribution	Assumes that scatterers are uniformly distributed within an angle distribution of θ_{BW} and a radial range of ΔR centered about the mobile Magnitude and phase associated with each scatterer are selected at random from a uniform distribution of [0,1] and [0, 2π], respectively	[26]
Modified Saleh-Valenzuela's Model	An extension to the Saleh-Valenzuela model, including AOA information in the channel model Assumes that time and the angle are statistically independent Based on indoor measurements	[28]
Extended Tap-Delay-Line Model	Wideband channel model Extension of the traditional statistical tap-delay-line model which includes AOA information The joint density functions of the model parameters should be determined from measurements	[29]
Spatio-Temporal Model (Lu, Lo, and Litva's Model)	Model of multipath propagation based on the distribution of the scatterers in elliptical subregions, corresponding to a range of excess delay time Similar to the GBSBEM	[30]
Measurement-Based Channel Model	Parameters are based on measurement Characterizes the propagation environment in terms of scattering points	[32]
Ray Tracing Models	Deterministic model based on the geometric theory and reflection, diffraction, and scattering models Uses site-specific information, such as building databases or architecture drawings	[33–36]

Table 3. *Summary of spatial channel models.*

$$\text{Relative Angle Change (\%)} = 100 \times \sqrt{1 - \left| \frac{\mathbf{a}_i^*}{\|\mathbf{a}_i\|} \cdot \frac{\mathbf{a}_j^*}{\|\mathbf{a}_j\|} \right|^2}$$

and the relative amplitude change, found using

$$\text{Relative Amplitude Change(dB)} = 20\log_{10} \frac{\|\mathbf{a}_j\|}{\|\mathbf{a}_i\|}$$

where $\mathbf{a}_i$ and $\mathbf{a}_j$ are the two spatial signatures (array response vectors) being compared. The measurements indicate that when the mobile and surroundings are stationary, there are relatively small changes in the spatial signature. Likewise, there are moderate changes when objects and the environment are in motion and large changes when the mobile itself is moving. Also, it was found that the spatial signature changes significantly with a change in carrier frequency. In particular, the measurements found that the relative amplitude change in the spatial signal could exceed 10 dB with a frequency change of only 10 MHz. This result indicates that the uplink spatial signature cannot be directly applied for downlink beamforming in most of today's cellular and PCS systems that have 45 MHz and 80 MHz separation between the uplink and downlink frequencies, respectively.

Application of Spatial Channel Models

The effect that classical channel properties such as delay spread and Doppler spread have on system performance has been an active area of research for several years and hence is fairly well understood. The spatial channel models include the AOA properties of the channel, which are often characterized by the angle spread. The angle spread has a major impact on the correlation observed between the pairs of elements in the array. These correlation values specify the received signal vector covariance matrix, which is known to determine the performance of linear combining arrays [44]. In general, the higher the angle spread the lower the correlation observed between any pair of elements in the array. The various spatial channel models provide different angle spreads and hence will predict different levels of system performance.

The channel models presented here have various applications in the analysis and design of systems that utilize adaptive antenna arrays. Some of the models were developed to provide analytical models of the spatial correlation function, while others are intended primarily for simulation purposes.

Simulation

More and more companies are relying on detailed simulations to help design and develop today's wireless networks. The application of adaptive antennas is no exception. However, to obtain reliable results, accurate spatial channel models are needed. With accurate simulations of adaptive antenna array systems, researchers will be able to predict the capacity improvement, range extension, and other performance measures of the system, which in turn will determine the cost effectiveness of adaptive array technologies.

Algorithm Development

The availability of channel models also opens up the possibility of developing new maximum likelihood smart antennas and AOA estimation algorithms based on these channel models. Good analytical models that will provide insights into the structure of the spatial channel are needed.

Conclusions

As antenna technology advances, radio system engineers are increasingly able to utilize the spatial domain to enhance system performance by rejecting interfering signals and boosting desired signal levels. However, to make effective use of the spatial domain, design engineers need to understand and appropriately model spatial domain characteristics, particularly the distribution of scatterers, angles of arrival, and the Doppler spectrum. These characteristics tend to be dependent on the height of the transmitting and receiving antennas relative to the local environment. For example, the distributions expected in a microcellular environment with relatively low base station antenna heights are usually quite different from those found in traditional macrocellular systems with elevated base station antennas.

This article has provided a review of a number of spatial propagation models. These models can be divided into three groups:

- General statistically based models
- More site-specific models based on measurement data
- Entirely site-specific models.

The first group of models (Lee's Model, Discrete Uniform Distribution Model, Geometrically Based Single Bounce Statistical Model, Gaussian Wide Sense Stationary Uncorrelated Scattering Model, Gaussian Angle of Arrival Model, Uniform Sectored Distributed Model, Modified Saleh-Valenzuela's Model, Spatio-Temporal Model) are useful for general system performance analysis. The models in the second group (Extended Tap Delay Line Model and Measurement-Based Channel Model) can be expected to yield greater accuracy but require measurement data as an input. An example from the third group of models is Ray Tracing, which has the potential to be extremely accurate but requires a comprehensive description of the physical propagation environment as well as measurements to validate the models.

Further research is required to validate and enhance the models described in this article. Bearing in mind that an objective of modeling is to substantially reduce the amount of physical measurement required in the system planning process, it is important for design engineers to have reliable models of AOA, TDOA, delay spread, and the power of the multipath components. Further measurement programs that focus on spatial domain signal characteristics are required. These programs would greatly benefit from the development of improved measurement equipment.

Armed with improved spatial channel modeling tools and a greater understanding of signal propagation, engineers can begin to meet the challenges inherent in designing future high-capacity/high-quality wireless communication systems, including the effective use of smart antennas.

References

[1] R. H. Clarke, "A Statistical Theory of Mobile-Radio Reception," *Bell Sys. Tech. J.*, vol. 47, 1968, pp. 957–1000.

[2] M. J. Gans, "A Power Spectral Theory of Propagation in the Mobile Radio Environment," *IEEE Trans. Vehic. Tech.*, vol.VT-21, Feb. 1972, pp. 27–38.

[3] W. C. Y. Lee, *Mobile Communications Engineering*, New York: McGraw Hill, 1982.

[4] Turin, "A Statistical Model for Urban Multipath Propagation," *IEEE Trans. Vehic. Tech.*, vol. VT-21, no. 1, Feb. 1972, pp. 1–11.

[5] T. S. Rappaport, *Wireless Communications: Principles & Practice*, Upper SaddleRiver, NJ: Prentice Hall PTR, 1996.

[6] F. Adachi *et al.*, "Crosscorrelation Between the Envelopes of 900 MHz Signals Received at a Mobile Radio Base Station Site," *IEE Proc.*, vol. 133, Pt. F, no. 6, Oct. 1986, pp. 506–12.

[7] J. D. Parsons, *The Mobile Radio Propagation Channel*, New York: John Wiley & Sons, 1992.

[8] W. C. Y. Lee, *Mobile Cellular Telecommunications Systems*, New York: McGraw Hill, 1989.

[9] D. Aszetly, "On Antenna Arrays in Mobile Communication Systems: Fast Fading and GSM Base Station Receiver Algorithms," Ph.D. dissertation, Royal Inst. Technology, Mar. 1996.
[10] S. P. Stapleton, X. Carbo, and T. McKeen, "Spatial Channel Simulator for Phased Arrays," *Proc. IEEE VTC.*, 1994, pp 1789–92.
[11] S. P. Stapleton, X. Carbo, and T. Mckeen, "Tracking and Diversity for a Mobile Communications Base Station Array Antenna," *Proc. IEEE VTC*, 1996, pp. 1695–99.
[12] R. B. Ertel, "Vector Channel Model Evaluation," Tech.rep., SW Bell Tech. Resources, Aug. 1997.
[13] J. William C. Jakes, ed., *Microwave Mobile Communications*, New York: John Wiley & Sons, 1974.
[14] P. Petrus, "Novel Adaptive Array Algorithms and Their Impact on Cellular System Capacity," Ph.D. dissertation, Virginia Polytechnic Inst. and State Univ., Mar. 1997.
[15] P. Petrus, J. H. Reed, and T. S. Rappaport, "Effects of Directional Antennas at the Base Station on the Doppler Spectrum," *IEEE Commun. Lett.*, vol. 1, no. 2, Mar. 1997.
[16] R. B. Ertel, "Statistical Analysis of the Geometrically Based Single Bounce Channel Models," unpublished notes, May 1997.
[17] J. C. Liberti, "Analysis of CDMA Cellular Radio Systems Employing Adaptive Antennas," Ph.D. dissertation, Virginia Polytechnic Inst. and State Univ., Sept. 1995.
[18] J. C. Liberti and T. S. Rappaport, "A Geometrically Based Model for Line of Sight Multipath Radio Channels," *IEEE VTC*, Apr. 1996, pp. 844–48.
[19] P. Zetterberg and B. Ottersten, "The Spectrum Efficiency of a Basestation Antenna Array System for Spatially Selective Transmission," *IEEE VTC*, 1994.
[20] P. Zetterberg, "Mobile Communication with Base Station Antenna Arrays: Propagation Modeling and System Capacity," Tech. rep., Royal Inst. Technology, Jan. 1995.
[21] P. Zetterberg and P. L. Espensen, "A Downlink Beam Steering Technique for GSM/DCS1800/PCS1900," IEEE PIMRC, Taipei, Taiwan, Oct., 1996.
[22] P. Zetterberg, P. L. Espensen, and P. Mogensen, "Propagation, Beamsteering and Uplink Combining Algorithms for Cellular Systems," ACTS Mobile Commun. Summit, Granada, Spain, Nov., 1996.
[23] B. Ottersten, "Spatial Division Multiple Access (SDMA) in Wireless Communications," *Proc. Nordic Radio Symp.*, 1995.
[24] G. G. Raleigh and A. Paulraj, "Time Varying Vector Channel Estimation for Adaptive Spatial Equalization," *Proc. IEEE Globecom*, 1995, pp. 218–24.
[25] P. Mogensen *et al.*, "Algorithms and Antenna Array Recommendations," Tech.rep. A020/AUC/A12/DR/P/1/xx-D2.1.2, Tsunami (II), Sept. 1996.
[26] O. Norklit and J. B. Anderson, "Mobile Radio Environments and Adaptive Arrays," *Proc. IEEE PIMRC*, 1994, pp. 725–28.
[27] A. M. Saleh and R. A. Valenzuela, "A Statistical Model for Indoor Multipath Propagation," *IEEE JSAC*, vol. SAC-5, Feb. 1987.
[28] Q. Spencer *et al.*, "A Statistical Model for Angle of Arrival in Indoor Multipath Propagation," *IEEE VTC*, 1997, pp 1415–19.
[29] A. Klein and W. Mohr, "A Statistical Wideband Mobile Radio Channel Model Including the Direction of Arrival," *Proc. IEEE 4th Int'l. Symp. Spread Spectrum Techniques & Applications*, 1996, pp. 102–06.
[30] M. Lu, T. Lo, and J. Litva, "A Physical Spatio-Temporal Model of Multipath Propagation Channels," *Proc. IEEE VTC*, 1997, pp. 180–814.
[31] E. S. Sousa *et al.*, "Delay Spread Measurements for the Digital Cellular Channel in Toronto," *IEEE Trans. Vehic. Tech.*, vol. 43, no. 4, Nov. 1994, pp. 837–47.
[32] J. J. Blanz, A. Klein, and W. Mohr, "Measurement-Based Parameter Adaptation of Wideband Spatial Mobile Radio Channel Models," *Proc. IEEE 4th Int'l. Symp. Spread Spectrum Techniques & Applications*, 1996, pp. 91–97.
[33] K. R. Schaubach, N. J. Davis IV, and T. S. Rappaport, "A Ray Tracing method for Predicting Path Loss and Delay Spread in Microcellular Environment," *IEEE VTC*, May 1992, pp. 932–35.
[34] J. Rossi and A. Levi, "A Ray Model for Decimetric Radiowave Propagation in an Urban Area," *Radio Science,* vol. 27, no. 6, 1993, pp. 971–79.
[35] R. A. Valenzuela, "A Ray Tracing Approach for Predicting Indoor Wireless Transmission," *IEEE VTC*, 1993, pp. 214–18.
[36] S. Y. Seidel and T. S. Rappaport, "Site-Specific Propagation Prediction for Wireless In-Building Personal Communication System Design," *IEEE Trans. Vehic. Tech.*, vol. 43, no. 4, Nov. 1994.
[37] P. Petrus, J. H. Reed, and T. S. Rappaport, "Geometrically Based Statistical Channel Model for Macrocellular Mobile Environments," *IEEE Proc. GLOBECOM, 1996*, pp. 1197–1201.
[38] A. Klein *et al.*, "Direction-of-Arrival of Partial Waves in Wideband Mobile Radio Channels for Intelligent Antenna Concepts," *IEEE VTC*, 1996, pp. 849–53.
[39] H. J. Thomas, T. Ohgane, and M. Mizuno, "A Novel Dual Antenna Measurement of the Angular Distribution of Received Waves in the Mobile Radio Environment as a Function of Position and Delay Time," *Proc. IEEE VTC*, vol. 1, 1992, pp 546–49.
[40] Q. Spencer *et al.*, "Indoor Wideband Time/Angle of Arrival Multipath Propagation Results," *IEEE VTC*, 1997, pp. 1410–14.
[41] J. Fuhl, J-P Rossi, and E. Bonek, "High Resolution 3-D Direction-of-Arrival Determination for Urban Mobile Radio," *IEEE Trans. Antennas and Propagation*, vol. 45, no. 4, Apr. 1997, pp. 672–81.
[42] M. D. Zoltowski, M. Haardt, and C. P. Mathews, "Closed-Form 2-D Angle Estimation with Rectangular Arrays in Element Space or Beamspace via Unitary ESPRIT," *IEEE Trans. Signal Processing*, vol., vol. 44, Feb. 1996, pp. 316–28.
[43] S. S. Jenget *et al.*, "Measurements of Spatial Signature of an Antenna Array," *Proc. IEEE 6th PIMRC*, vol. 2, Sept. 1995, pp. 669–72.
[44] R. A. Monzingo and T. W. Miller, *Introduction to Adaptive Arrays*, New York: John Wiley & Sons, 1980.

Additional Reading

[1] M. J. Devasirvatham, "A Comparison of Time Delay Spread and Signal Level Measurements with Two Dissimilar Office Buildings," *IEEE Trans. Antennas and Propagation*, vol. AP-35, No. 3, Mar. 1994, pp. 319–24.
[2] M. J. Feuerstein *et al.*, "Path Loss, Delay Spread, and Outage Models as Functions of Antenna for Microcellular Systems Design," *IEEE Trans. Vehic. Tech.*, vol. 43, no. 3, Aug. 1994, pp. 487–98.
[3] J. C. Liberti and T. S. Rappaport, "Analytical Results for Capacity Improvements in CDMA," *IEEE Trans. Vehic. Tech.*, VT-43, no. 3, Aug. 1994.
[4] D. Molkdar, "Review on Radio Propagation into and within Buildings," *IEE Proc.*, vol. 138, no. 1, Feb. 1991.
[5] A. F. Naguib, A. Paulraj, and T. Kailath, "Capacity Improvement with Base-Station Antenna Array," *IEEE Trans. Vehic. Tech.*, VT-43, no. 3, Aug. 1994, pp. 691–98.
[6] A. F. Naguib and A. Paulraj, "Performance Enhancement and Trade-offs of a Smart Antenna in CDMA Cellular Network," *IEEE VTC*, 1995, pp. 225–29.
[7] S. Y. Seidel *et al.*, "Path Loss, Scattering and Multipath Propagation Statistics for European Cities for Digital Cellular and Microcellular Radiotelephone," *IEEE Trans. Vehic, Tech,*, vol. VT-40, no. 4, Nov. 1991, pp. 721–30.
[8] S. C. Swales, M. A. Beach, and J. P. MacGeehan, "The Performance Enhancement of Multi-beam Adaptive Base-station Antenna for Cellular Land Mobile Radio System," *IEEE Trans. Vehic. Tech.*, vol.VT-39, Feb. 1990, pp. 56–67.

Biographies

RICHARD B. ERTEL received his Associate of Arts in engineering from Harrisburg Area Community College in 1991 with highest distinction. He then received his B.S.E.E. with highest honors and M.S.E.E. degrees from Penn State University in May 1993 and May 1996, respectively. He is currently a Bradley Fellow and research assistant at Virginia Tech.

PAULO CARDIERI received a B.S. degree from Maua School of Engineering, Sao Caetano do Sul, in 1987, and an M.Sc. degree from the State University of Campinas, Campinas, SP, in 1994, both in electrical engineering. He is currently pursuing a Ph.D. degree in electrical engineering at Virginia Tech. Since 1987, he has been with the Research and Development Center of the Brazilian Telecommunication Company (CPqD-TELEBRAS) (on leave). From November 1991 to August 1992 he was visiting researcher at Centro Studi e Laboratori Telecomunicazioni, Turin, Italy, working on equalization techniques for digital mobile systems.

KEVIN W. SOWERBY [M '90] received B.E. and Ph.D. degrees in electrical and electronic engineering at the University of Auckland, Auckland, New Zealand in 1986 and 1989, respectively. During 1989 and 1990 he was a Leverhulme Visiting Fellow at the University of Liverpool, United Kingdom, in the Department of Electrical Engineering and Electronics. In 1990 he returned to the University of Auckland to take up a lectureship in the Department of Electrical and Electronic Engineering, where he is currently a senior lecturer. During 1997 he has been on research and study leave as a visitor at both Virginia Tech, United States, and Simon Fraser University, B.C., Canada.

THEODORE S. RAPPAPORT [F '98] received B.S.E.E., M.S.E.E., and Ph.D. degrees from Purdue University in 1982, 1984, and 1987, respectively. Since 1988 he has been on the Virginia Tech electrical and computer engineering faculty, where he is the James S. Tucker Professor, and founder and director of the Mobile and Portable Radio Research Group (MPRG), a university research and teaching center dedicated to the wireless communications field. In 1989 he founded TSR Technologies, Inc. a cellular radio/PCS manufacturing firm sold in 1993.

JEFFREY H. REED is an associate professor and associate director of the MPRG at Virginia Tech. He is also a member of the Center for Wireless Telecommunications. He received his B.S.E.E. in 1979, M.S.E.E. in 1980, and Ph.D. in 1987, all from the University of California, Davis. From 1980 to 1986, he worked for Signal Science, Inc., a small consulting firm specializing in DSP and communication systems. After graduating with his Ph.D., he worked as a private consultant and a part-time faculty member at the University of California, Davis. In August 1992, he joined the faculty of the Bradley Department of Electrical Engineering at Virginia Tech.